

Soft mode in cubic PbTiO₃ by hyper-Raman scatteringJ. Hlinka,¹ B. Hehlen,² A. Kania,³ and I. Gregora¹¹*Institute of Physics, Academy of Sciences of the Czech Republic, Na Slovance 2, 18221 Praha 8, Czech Republic*²*Laboratoire des Colloïdes, Verres et Nanomatériaux (LCVN), UMR CNRS 5587, University of Montpellier II, 34095 Montpellier, France*³*Institute of Physics, University of Silesia, PL-40-007 Katowice, Poland*

(Received 27 November 2012; published 4 February 2013)

Hyper-Raman scattering experiments allowed collecting the spectra of the lowest F_{1u} -symmetry mode of PbTiO₃ crystal in the paraelectric phase up to ≈ 930 K as well as down to about 1 K above the phase transition. It is realized that this mode is fully responsible for the Curie-Weiss behavior of its dielectric permittivity above T_c . Near the phase transition, this phonon frequency softens down to 17 cm^{-1} and its spectrum can be well modeled as a response of a single damped harmonic oscillator. It is concluded that PbTiO₃ constitutes a clean example of a soft-mode-driven ferroelectric system.

DOI: [10.1103/PhysRevB.87.064101](https://doi.org/10.1103/PhysRevB.87.064101)

PACS number(s): 77.80.-e, 78.30.-j, 63.20.-e, 77.80.B-

Since the seminal works of Frohlich, Ginzburg, Cochran, and Landauer,¹⁻⁵ it is well understood that high dielectric constant of many practically exploited polar materials is directly related to the presence of a low-frequency polar excitation through the Lyddane-Sachs-Teller relationship. In displacive-type ferroelectrics, this excitation has a character of a vibrational lattice mode, so-called soft mode. Soft-mode frequencies are typically found in the 0.1–1 THz frequency range, so that the high permittivity persists throughout the whole megahertz-gigahertz range, and it is usually quite a robust intrinsic property. Other materials may reveal high static permittivities also for other reasons, for example, due to mobile ferroelectric domain walls, space-limited conductivity at various structural inhomogeneities, etc.⁶⁻⁸ As a rule, such mechanisms usually lead to high permittivities only at very low frequencies, and the dielectric properties of these materials are also much more susceptible to various fatigue phenomena. Therefore the terahertz-range frequency dispersion of the dielectric permittivity provides the key information needed to understand the potential of practical use of the high-permittivity materials.

A nice example of a material owing its high permittivity to a well-defined terahertz-range frequency polar vibration is the quantum paraelectric SrTiO₃.^{9,10} In most of its ferroelectric counterparts, however, soft polar fluctuations cannot not be described by a single damped harmonic oscillator (DHO).¹¹ In fact, it is tempting to conclude that there is some kind of additional central mode in the vicinity of all ferroelectric phase transitions. At least, additional terahertz range excitations related to the soft phonon degree of freedom have been quite neatly experimentally identified in rather different perovskite polar materials, such as tetragonal ferroelectric BaTiO₃,¹² on one hand and in a pseudocubic relaxor ferroelectric PbMg_{1/3}Nb_{2/3}O₃,¹³ on the other hand. Seemingly similar phenomena may probably be of a rather different nature, but in both cases, the presence of the additional excitation in the dielectric spectrum is crucial for explaining the magnitudes of the measured static permittivity.

Therefore it seems also important to provide clean examples of ferroelectric materials where the terahertz range permittivity is actually well described by a single polar soft-mode excitation. Originally, the paraelectric PbTiO₃ has been considered

as the example of such a simple soft-mode system.¹⁴ The presence of a central peak was later proposed to exist there as well, but only in a gigahertz frequency range.¹⁵⁻¹⁷ In reality, the measurements of the soft-mode spectra above the, fairly high, ferroelectric phase transition temperature ($T_c = 760$ K) of PbTiO₃ turned out to be technically quite challenging. Already the pioneering inelastic neutron scattering (INS) study of Shirane *et al.*¹⁴ reported that accurate measurements in the vicinity of the Brillouin zone center are difficult and the data reported there are, in fact, extrapolated from phonon dispersion relations. Similar difficulties have been encountered in subsequent INS experiments^{18,19} and, even less straightforward, is the analysis of the confocal Raman light scattering spectra reported in Ref. 20.

In fact, there are quite sizable disagreements among the published estimates for soft-mode frequency and its temperature dependence in the paraelectric phase. For example, the extrapolation of the soft-mode frequency to the phase transition temperature gives about 11 cm^{-1} according to Ref. 19, 20 cm^{-1} according to Ref. 14, and more than 60 cm^{-1} according to Ref. 20.

The aim of this paper is to report a new set of reference spectral data in the vicinity of a ferroelectric phase transition, demonstrating that the paraelectric PbTiO₃ can be indeed considered as such a clean case where the terahertz response can be well modeled by a single DHO.

A clear-cut answer to these issues was obtained here by means of Hyper-Raman scattering (HRS). Previously, soft modes has been studied by this technique in a range of polar perovskite materials.²¹⁻²³ In principle, state-of-art instrumental resolution allows measurements of polar modes in the paraelectric phase by HRS down to a few reciprocal centimeters. Present HRS experiments have been performed using the setup described in Ref. 23, only upgraded with an optical microscope.

The sample was a 1-mm thick platelet of a PbTiO₃ single crystal grown at University of Silesia,²⁴ with a natural surface normal to the [001] (z axis). It was mounted in a hot stage with the [100] (x) and [010] (y) crystallographic axes parallel to the horizontal (H) and vertical (V) direction, respectively. The data were collected in the backscattering geometry with $q \parallel [001]$. A broadband half-wave plate followed by a

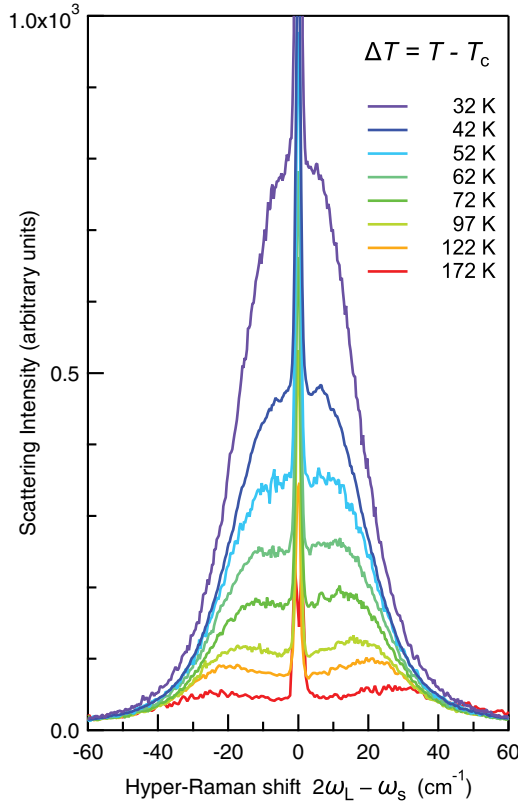


FIG. 1. (Color online) Unpolarized (V + H) HRS spectra of the paraelectric phase of PbTiO₃ single crystal for several temperatures indicated in the figure with respect to the phase transition ($T_C \approx 760$ K). These spectra are not corrected for temperature factor.

Glan-Thomson polarizer allowed for analysis of the scattered light polarized along V or H. A 1800 grooves/mm grating and a 150- μ m entrance slit give rise to a spectral resolution of ~ 3 cm⁻¹. Cooling and heating rates did not exceed 10 K/min with a temperature stabilized within $\sim \pm 1$ K. Since the strong SHG signal in the ferroelectric phase persists up to the phase transition T_C , the soft-mode spectra could be measured only in the paraelectric phase. On the other hand, the onset of SHG and Raman scattering at T_C allowed us to determine quite precisely the measured temperatures with respect to T_C .

The simple O_h^1 ($Z = 1$) perovskite structure of paraelectric PbTiO₃ has four zone center optic modes, three F_{1u} polar modes and one F_{2u} nonpolar vibration, all being triply degenerate and active in HRS. The lowest frequency F_{1u} is known to play the role of the soft mode. A representative set of resulting HRS spectra revealing this mode is shown in Fig. 1. All these spectra show a broad soft-mode response and a resolution-limited central line. Up to about 50 K above T_C , the broad soft mode gives a bell-like response centered at zero energy. Above this temperature, the response function clearly shows two broad maxima, corresponding to the Stokes and anti-Stokes spectral bands.

The narrow central line probably contains both surface sensitive elastic and resolution-limited quasielastic scattering, so that we focused here on the analysis of the broad, phonon part of the spectrum. In fact, at all temperatures, this part of the spectrum could be nicely adjusted to the model of a single DHO, see Fig. 2. Strictly speaking, the measured intensity was

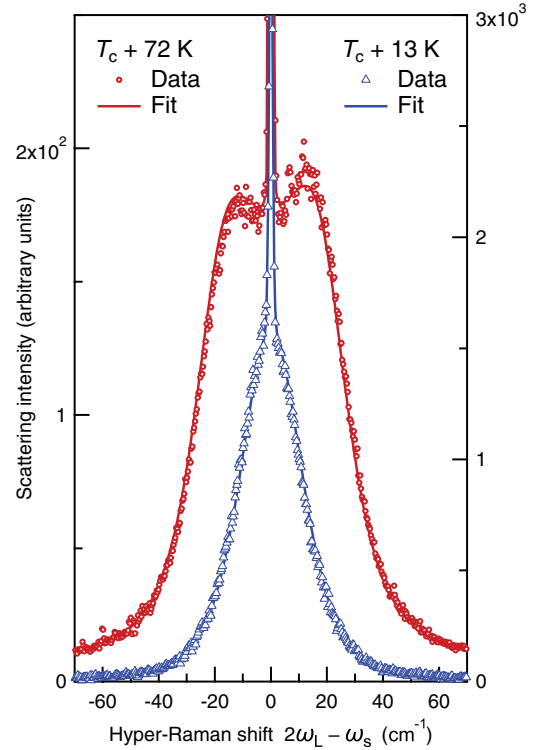


FIG. 2. (Color online) Unpolarized (V + H) HRS spectra of PMN at 13 and 72 K above the phase transition ($T_C \approx 760$ K) adjusted to the model of DHO. The resolution limited central line is adjusted by a narrow Gaussian peak.

adjusted to the sum of a flat background, a narrow Gaussian peak standing for the resolution limited central line and the standard one-phonon scattering lineshape model²⁵

$$I_{\text{HRS}} \propto \left(\frac{\omega_S^4}{\omega}\right) [n(\omega) + 1] F(\omega) \sum_{\delta} |e_i^S R_{ijk}^{\delta} e_j^L e_k^L|^2, \quad (1)$$

where $\omega_S = 2\omega_L \pm \omega$ is the frequency of the scattered field, $n(\omega)$ is the Bose-Einstein population factor, e^L and e^S are the polarization vectors of the incident (L) and detected (S) photons, respectively, the index δ distinguishes different HRS tensors R_{ijk}^{δ} of a degenerate mode, and $F(\omega)$ is the normalized response function of the mode described by

$$F(\omega) = (2\omega/\pi) \text{Im}[1/(\omega_0^2 - \omega^2 - i\Gamma\omega)], \quad (2)$$

where ω_0 and Γ are DHO frequency and damping, respectively.

The resulting least-squares fit values of ω_0^2 as a function of temperature are displayed in Fig. 3. This temperature dependence is visibly fairly linear, and its adjustment to Cochran law $\omega_0^2 = A(T - T_{\text{SM}})$ provides $A = 5$ cm⁻²K⁻¹ and $T_{\text{SM}} = T_C - 55$ K. The value of Γ parameter has shown only a very small variation (from about 35 cm⁻¹ at $T_C + 2$ K to about 30 cm⁻¹ at $T_C + 172$ K). Nevertheless, the value of Γ is comparable with the soft-mode frequency itself (ω_0 determined from the present experiments extrapolates to ~ 17 cm⁻¹ at T_C). Therefore we have also shown in Fig. 3 the two auxiliary frequency parameters $\omega' = \sqrt{\omega_0^2 - \Gamma^2/2}$ and $\omega'' = \sqrt{\omega_0^2 - \Gamma^2/4}$. The former quantity gives the position of the maximum of the one-phonon DHO scattering spectral function of Eq. (2) in the high-temperature limit ($kT \gg \hbar\omega_0$)

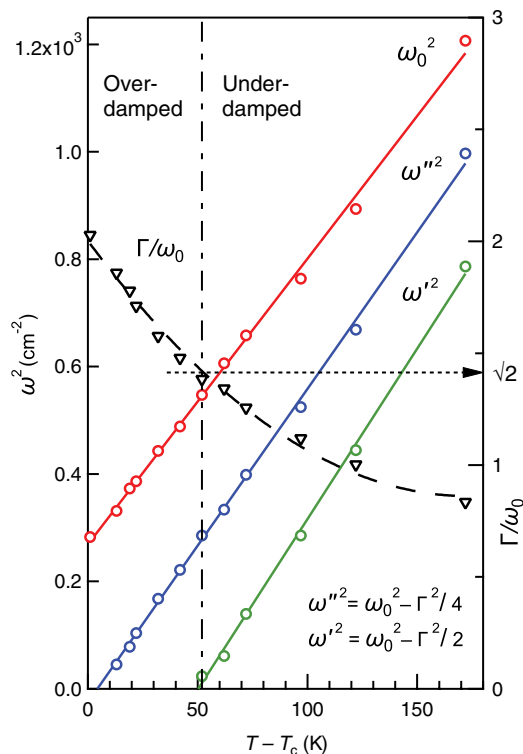


FIG. 3. (Color online) Temperature evolution of soft-mode spectral parameters in the paraelectric phase of PbTiO₃. Temperature dependence of the soft-mode frequency squared (ω_0^2) was adjusted to a linear (Cochran) law discussed in the text (full line). The quantities ω''^2 and ω'^2 show analogous behavior. The vertical lines indicated crossover between overdamped and underdamped soft-mode regimes. Triangle symbols stand for the relative soft-mode damping, which is the ratio of damping and soft-mode frequency Γ/ω_0 . These data correspond to the right-hand side scale.

as long as the DHO is underdamped ($\omega_0 > \Gamma/\sqrt{2}$). It is clear from Fig. 3 that the overdamped/underdamped crossover temperature T_{OD} at which ω'^2 approaches zero is at about 50 K above T_C .

The latter quantity, preferred over ω_0 by some authors,²⁰ defines the periodic factor in the temporal response of the oscillator coordinate Q in the absence of driving forces $Q(t) = \exp^{-t\Gamma/2} \cos(\omega''t + \phi)$ for ($\omega_0 > \Gamma/2$). Accidentally, ω'^2 happens to extrapolate to zero quite close to T_C (see Fig. 3).

We have noted that the present values of ω_0 reported in Fig. 3 fall within the error bars of the corresponding values measured by INS in a recent paper by Tomeno *et al.*¹⁹ The frequencies deduced from the original work of Shirane *et al.*¹⁴ are a bit higher but still in a reasonable agreement with the present experiment. An independent attempt to determine paraelectric soft-mode frequency with the INS technique was reported by Kempa *et al.*¹⁸ Values estimated there implied even higher soft-mode frequencies. We now believe that the main source of differences among these INS data is the effect of momentum resolution, which was somewhat coarser in the experiment of Ref. 18. The soft-mode dispersion of PbTiO₃ is indeed very steep,¹⁹ so that the admixture of the response of the modes with the phonon wave vectors away from the Brillouin zone center could considerably upshift the apparent zone

center frequency. Another possibility could be the presence of oxygen or lead vacancies in the sample (as mentioned in Ref. 19) but since the sample used in the present HRS measurements was prepared under similar conditions as that of the Ref. 18, it seems less likely.

The paraelectric soft-mode frequency of PTO was also recently deduced from confocal Raman scattering spectra in Ref. 20. However, the paraelectric soft mode is not active in Raman scattering, so that the measured spectral data did not originate from a standard first-order scattering. The theoretical analysis of Ref. 20, inspired by the idea of defect-induced Raman scattering is most likely not appropriate for a qualitative determination of the soft-mode parameters at all, as the data obtained there are in a very strong disagreement with the present measurement; the soft-mode frequencies obtained in Ref. 20 are even higher than that of the INS estimates of Ref. 18.

The Cochran constant from the present experiments ($5 \text{ cm}^{-2}\text{K}^{-1}$) has the lowest value among the reported ones (about $8.4 \text{ cm}^{-2}\text{K}^{-1}$ is obtained in Refs. 14 and 19, and about $35 \text{ cm}^{-2}\text{K}^{-1}$ is provided in Ref. 20). The latter estimate is probably biased by the very indirect analysis of the cubic phase Raman spectra, while the somewhat higher values reported in Refs. 14 and 19 could be perhaps related to a broader temperature interval in which the soft mode was followed (INS data extended up to 1175 K in Ref. 19). Such a systematic dependence of the Cochran constant on the fitting temperature range could indicate a coupling of the soft mode to a central mode. On the other hand, the HRS and INS measurements both agree that the Cochran-law temperature T_0 is about 50 ± 15 K below the phase transition T_C . Present HRS data, taken in the same temperature region as the dielectric measurements, show that $T_C - T_0$ is close to 55 K, and so within the experimental uncertainty, the present Cochran-law temperature coincides with the temperature at which the inverse static susceptibility extrapolates to zero (the Curie-Weiss law extrapolating temperature T_{CW} of Ref. 26 is 43 K below T_C). Thus, although the present experiment could not directly probe the gigahertz range central peak in the paraelectric phase of PTO, we can conclude that if it exists, it has only a very small contribution to the static permittivity, and also the shift of the phase transition is much less than it was sometimes assumed.^{17,18}

In fact, this simple soft-mode picture is also consistent with the observed relative change of the permittivity at the phase transition. Probably, the most reliable megahertz-range dielectric data of Ref. 27 suggest that at the phase transition, the paraelectric permittivity ϵ is about ten times larger than the axial ferroelectric permittivity ϵ_{33} ($\epsilon/\epsilon_{33} \approx 10$). From the LST relation, assuming that only the soft-mode frequency has changed at the transition, the same ratio could be expressed as $\omega_{A_1}^2/\omega_{SM}^2$, where ω_{A_1} is the frequency of the soft mode in the ferroelectric phase. Indeed, the present HRS value of $\omega_{SM} \approx 17 \text{ cm}^{-1}$ together with the earlier measured^{16,28} values of $\omega_{A_1} \approx 60 \text{ cm}^{-1}$ leads us also to the ratio of $\omega_{A_1}^2/\omega_{SM}^2 \approx 10$.

Finally, it is interesting to compare soft-mode spectra of PbTiO₃ with those of similar ferroelectric compounds like BaTiO₃. From the symmetry point of view, the ferroelectric transition in both compounds is identical; in both cases, the paraelectric cubic perovskite $Pm\bar{3}m$ ($Z = 1$) phase transforms

to the tetragonal ferroelectric $P4mm$ ($Z = 1$) phase. However, the soft-mode dynamics is markedly different. Even though the phase transition in BaTiO_3 occurs at much lower temperature ($T_C \approx 400$ K), all attempts to fit the paraelectric soft-mode spectrum with a simple DHO yielded an overdamped phonon (the resulting Γ/ω was greater than $\sqrt{2}$ at all temperatures investigated).³⁴ Moreover, the recent experiments and material-specific theoretical calculations^{12,29–31,33} are giving a fairly convincing evidence in favor of the old but for long-time questioned idea^{21,34,35} that in the vicinity of the transition temperature, the adequate description of the soft-mode spectrum of BaTiO_3 requires a two-mode model, rather than just a single DHO formula. The existence of such

additional soft-mode spectral component, often denoted as a (spectrally) broad central mode, has been even more obvious in some other related compounds, such as, for example, in SrTiO_3 , KTaO_3 or $(\text{Ba}_{0.5}\text{Sr}_{0.5})\text{TiO}_3$.^{32,36–38} At the same time, there is no evidence for such additional broad central mode in case of PbTiO_3 , at least not in the fairly wide spectral range investigated in the present experiment. Because of these differences, we can conclude that the PbTiO_3 can be considered as a very important model case of purely soft-mode-driven ferroelectric transition.

This work has been supported by the Czech Ministry of Education (Project MSMT ME08109).

-
- ¹H. Fröhlich, *Theory of Dielectrics* (Clarendon Press, Oxford, 1949).
²V. L. Ginzburg, *Usp. Fiz. Nauk* **38**, 490 (1949).
³V. L. Ginzburg, *Zh. Eksp. Teor. Fiz.* **19**, 36 (1949).
⁴W. Cochran, *Phys. Rev. Lett.* **3**, 412 (1959).
⁵R. Landauer, *Ferroelectrics* **73**, 27 (1987).
⁶P. Lunkenheimer, V. Bobnar, A. V. Pronin, A. I. Ritus, A. A. Volkov, and A. Loidl, *Phys. Rev. B* **66**, 052105 (2002).
⁷J. Liu, C.-G. Duan, W.-G. Yin, W. N. Mei, R. W. Smith, and J. R. Hardy, *Phys. Rev. B* **70**, 144106 (2004).
⁸M. Li, Z. Shen, M. Nygren, A. Feteira, D. C. Sinclair, and A. R. West, *J. Appl. Phys.* **106**, 104106 (2009).
⁹A. S. Barker and M. Tinkham, *Phys. Rev.* **125**, 1527 (1962).
¹⁰G. Rupprecht and R. O. Bell, *Phys. Rev.* **125**, 1915 (1962).
¹¹J. Petzelt, G. V. Kozlov, and A. A. Volkov, *Ferroelectrics* **73**, 101 (1987).
¹²J. Hlinka, T. Ostapchuk, D. Nuzhnyy, J. Petzelt, P. Kuzel, C. Kadlec, P. Vanek, I. Ponomareva, and L. Bellaïche, *Phys. Rev. Lett.* **101**, 167402 (2008).
¹³A. Al-Zein, J. Hlinka, J. Rouquette, and B. Hehlen, *Phys. Rev. Lett.* **105**, 017601 (2010).
¹⁴G. Shirane, J. D. Axe, J. Harada, and J. P. Remeika, *Phys. Rev. B* **2**, 155 (1970).
¹⁵M. D. Fontana, H. Idrissi, and K. Wojcik, *Europhys. Lett.* **11**, 419 (1990).
¹⁶M. D. Fontana, H. Idrissi, G. E. Kugel, and K. Wojcik, *J. Phys.: Condens. Matter* **3**, 8695 (1991).
¹⁷Y. Girshberg and Y. Yacoby, *Solid State Commun.* **103**, 425 (1997).
¹⁸M. Kempa, J. Hlinka, J. Kulda, P. Bourges, A. Kania, and J. Petzelt, *Phase Transitions* **79**, 351 (2006).
¹⁹I. Tomeno, J. A. Fernandez-Baca, K. J. Marty, K. Oka, and Y. Tsunoda, *Phys. Rev. B* **86**, 134306 (2012).
²⁰H. P. Soon, H. Taniguchi, Y. Fujii, M. Itoh, and M. Tachibana, *Phys. Rev. B* **78**, 172103 (2008).
²¹H. Presting, J. A. Sanjurjo, and H. Vogt, *Phys. Rev. B* **28**, 6097 (1983).
²²B. Hehlen, G. Simon, and J. Hlinka, *Phys. Rev. B* **75**, 052104 (2007).
²³A. Al-Zein, B. Hehlen, J. Rouquette, and J. Hlinka, *Phys. Rev. B* **78**, 134113 (2008).
²⁴A. Kania, A. Slodczyk, and Z. Ujma, *J. Cryst. Growth* **289**, 134 (2006).
²⁵H. Vogt, *Phys. Rev. B* **38**, 5699 (1988).
²⁶J. P. Remeika and A. M. Glass, *Mater. Res. Bull.* **5**, 37 (1970).
²⁷Z. Li, M. Grimsditch, C. M. Foster, and S.-K. Chan, *J. Phys. Chem. Solids* **57**, 1433 (1996).
²⁸H. M. Jang, M.-A. Oak, J.-H. Lee, Y. K. Jeong, and J. F. Scott, *Phys. Rev. B* **80**, 132105 (2009).
²⁹I. Ponomareva, L. Bellaïche, T. Ostapchuk, J. Hlinka, and J. Petzelt, *Phys. Rev. B* **77**, 012102 (2008).
³⁰G. Geneste, *Phys. Rev. B* **79**, 144104 (2009).
³¹E. K. H. Salje, M. A. Carpenter, G. F. Nataf, G. Picht, K. Webber, J. Weerasinghe, S. Lisenkov, and L. Bellaïche, *Phys. Rev. B* **87**, 014106 (2013).
³²Y. Yacoby and Y. Girshberg, *Phys. Rev. B* **77**, 064116 (2008).
³³S. Liu, L. Huang, J. Li, and S. O'Brien, *J. Appl. Phys.* **112**, 014108 (2012).
³⁴H. Vogt, J. A. Sanjurjo, and G. Rossbroich, *Phys. Rev. B* **26**, 5904 (1982).
³⁵K. Inoue and S. Akimoto, *Solid State Commun.* **46**, 441 (1983).
³⁶C. Kadlec, V. Skoromets, F. Kadlec, H. Nemeč, J. Hlinka, J. Schubert, G. Panaitov, and P. Kuzel, *Phys. Rev. B* **80**, 174116 (2009).
³⁷V. Skoromets, S. Glinsek, V. Bovtun, M. Kempa, J. Petzelt, S. Kamba, B. Malic, M. Kosec, and P. Kuzel, *Appl. Phys. Lett.* **99**, 052908 (2011).
³⁸J. Weerasinghe, L. Bellaïche, T. Ostapchuk, P. Kuzel, C. Kadlec, S. Lisenkov, I. Ponomareva, and J. Hlinka, [arXiv:1211.6970](https://arxiv.org/abs/1211.6970).